Stochastic multi-scale modelling of composite materials based on experimental data

A. Vanaerschot[1], S.V. Lomov[2], D. Moens[3], D. Vandepitte[1]
[1]Department of Mechanical Eng., Faculty of Engineering, KU Leuven, Leuven, Belgium
[2]Department of Metallurgy and Materials Eng., Faculty of Engineering, KU Leuven, Leuven, Belgium
[3]Department of Mechanical Eng., KU Leuven@Thomas More Mechelen, Mechelen, Belgium
email: Andy.Vanaerschot@mech.kuleuven.be, Stepan.Lomov@mtm.kuleuven.be,
David.Moens@mech.kuleuven.be, Dirk.Vandepitte@mech.kuleuven.be

ABSTRACT: Variability in textile composites is substantial. A full characterisation of the internal geometry supports material design and increases the reliability of numerical simulations. An approach is presented and tested to obtain a full statistical description of the internal structure of a carbon-epoxy 2/2 twill woven composite, produced using resin transfer moulding. In a first step experimental data are collected using micro-CT to characterise the short range, i.e. within unit cell dimensions, and optical imaging for the long range, spanning several unit cells. The statistical information of the tow reinforcement is quantified per tow type, warp and weft direction, in terms of standard deviation and correlation length. The largest variation is found for the in-plane tow centroid coordinate with a significantly different behaviour in warp and weft direction. Tow cross-sectional properties such as area and aspect ratio vary within the unit cell size with limited scatter. Cross-correlation between neighbouring tows is only observed for the in-plane position. In a second step the statistical data are the input for a multi-scale modelling strategy to generate virtual specimens with random tow reinforcement. While the mean trends of each tow property are directly taken from the experiments, the deviations are generated by two different geometry generators. The properties without cross-correlation are produced using a Markov Chain algorithm, while the cross-correlated in-plane coordinate is generated using the Karhunen-Loève series expansion. Virtual specimens are obtained which possess the same statistical information as present in the experimental samples.

KEY WORDS: Textile composites; Multi-scale modelling; Non-determinism; Probabilistic methods

1 INTRODUCTION

The internal geometry of fibre-based composites is subjected to a significant amount of variability, even for high-quality textiles. Besides the inadequacy of experimental data, methods are still lacking for reliable modelling of the effects of geometrical scatter on the randomness in the mechanical properties. The need for reliable numerical analysis of composite structures demands a realistic description of the tow reinforcement. A correct representation of the materials internal geometry and properties can only be achieved by [4]: (i) collecting enough experimental data on the spatially correlated random fluctuations of uncertain tow path parameters and (ii) deriving probabilistic information for the macroscopic properties from the lower scale mechanical characteristics.

This work presents the general approach and successive steps to build random virtual specimens, starting from the collection of experimental data till the generation of random samples. The methodology is applied on a typical woven textile composite.

2 COLLECTION OF EXPERIMENTAL DATA

2.1 Material

The tow reinforcement is a 2/2 twill woven Hexcel fabric (G0986 injectex) [1]. Carbon fibres are impregnated with expoy resin using Resin Transfer Moulding (RTM). The unit cell representation is given in Figure 1 with λ_x and λ_y the periods of the warp (x-direction) and weft (y-direction) tows. The nominal periodic lengths are 11.4 by 11.4 mm.

Two different sample configurations and non-destructive inspection techniques are applied to characterise the geometrical scatter on the short range, i.e. around unit cell dimensions, and the long range, i.e. exceeding the unit cell size. The short range statistical information is collected from an epoxy impregnated seven-ply stack-up using micro-CT, while the long range information is acquired by optical imaging of a one-ply 2/2 twill woven composite.

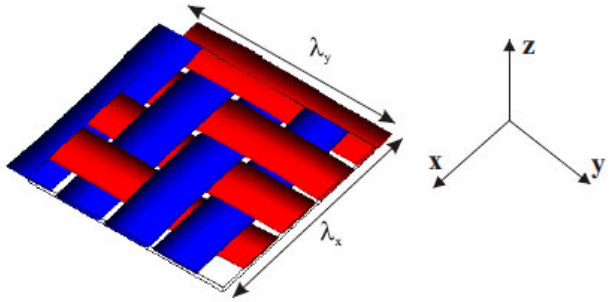

Figure 1. WiseTex [8] model of a 2/2 twill woven fabric.

2.2 Short range data

Statistical information of the internal geometrical variability at the short range is acquired using micro-CT. A sample of unit cell dimensions is positioned in a GE Nanotom of KU Leuven. A three-dimensional reconstructed volume is obtained and two-dimensional slices are extracted in warp and weft direction with a voxel size of $(6.75\ \mu m)^3$. Although the image quality of the cross-sections is optimised using

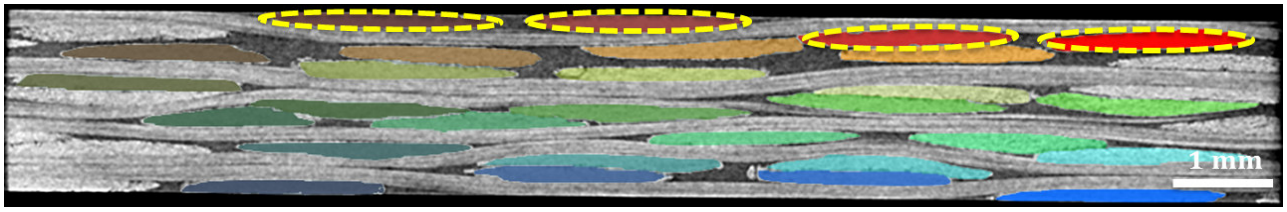

Figure 2. Digital image of a cross-section in weft direction obtained by micro-CT. Tows are identified by image segmentation and an elliptical shape is fitted to the tows in cross-section of ply 7.

different filtering techniques, fully-automated material segmentation is not possible. The similar material density of the carbon fibres and epoxy resin results in a low contrast, as can be seen from Figure 2. The required manual input for image segmentation limits the amount of slices to nineteen to analyse the structure of the sample in a reasonable time but capturing all the needed fluctuations in the tow path (set to every 0.75 mm along the tow path). The segmented tow shapes are fitted with an elliptical shape yielding information about the tow path centroids (ρ,z) with ρ=y for the warp tows and ρ=x for the weft tows, tow aspect ratio AR, tow area A and tow orientation θ in cross-section.

A statistical description of the tow reinforcement is obtained for each individual ply using the reference period collation method [2]. Tows that should be identical, given the nominal periodicity, are collected in one group that is called tow genus. All warp tows can be represented by a single genus and similar for the weft tows. The tow path parameters of each genus are described on an equidistant grid with spacing υ consisting of sixteen equally spaced points, with a total grid length set to the unit cell period of the particular genus (λ_x or λ_y). These periodic lengths are derived from the experimental data using a minimisation algorithm [9]. Characteristics of each tow parameter are decomposed into periodic systematic variations and non-periodic stochastic fluctuations. For ε representing one of the five parameters (ρ,z,AR,A,θ) and ρ=y or x respectively for warp and weft genus :

$$\varepsilon_i^{(j,t,p)} = \left\langle \varepsilon_i^{(j,t,p)} \right\rangle + \delta\varepsilon_i^{(j,t,p)} \qquad (1)$$

With $\delta\varepsilon_i^{(j,t,p)}$ the zero-mean deviation from the systematic value $< \varepsilon_i^{(j,t,p)} >$ at location i=1..16 along the tow j=1..4 of tow genus t= warp or weft in ply p=1..7. The average behaviour of the tow path is represented by the systematic trend, while the stochastic properties are expressed in terms of standard deviation and correlation length of the zero-mean deviations.

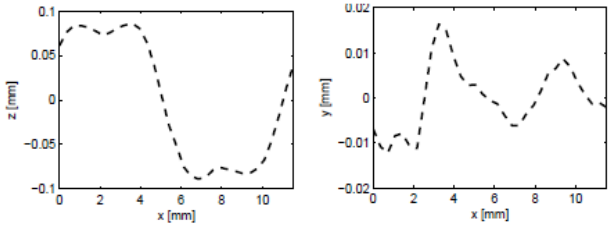

Figure 3. Sytematic trends of out-of-plane (left) and in-plane (right) centroid of the warp genus.

The presence of several plies maximises the data that can be derived from a single sample, but also permits to compare the statistics of each ply. Comparison of the ply systematic trends shows that no discernible differences are present for each single tow parameter. One warp and one weft systematic trend are enough to represent the mean tow path of a laminate. The systematic patterns of the out-of-plane and in-plane centroid of the warp genus are presented in Figure 3**.** The mean behaviour of the area, aspect ratio and orientation are correlated along the cross-over locations, with the overall mean values given in Table 1**.** Similar conclusions are made for the deviations from the systematic values. The statistics of the fluctuations for different plies are indistinguishable, permitting the derivation of the standard deviation and correlation length of each parameter using the data set of deviations combining data from all plies. This increase of data set size is favoured, certainly for the correlation information which is sensitive to the amount of data.

Table 1. Mean values for the tow cross-sectional properties.

	AR [-]	A [mm²]	θ [°]
Warp genus	12.95	0.37	-0.54
Weft genus	12.22	0.36	-1.27

The standard deviation of the tow parameters is presented in Table 2. The in-plane centroid coordinates for warp and weft genus exhibit the largest variability. This reflects the difference in tow tension for warp and weft tows during production.

Table 2. Experimental standard deviations.

	σ_x [mm]	σ_y [mm]	σ_z [mm]	σ_{AR} [-]	σ_A [mm²]	σ_θ [°]
Warp genus	-	0.113	0.014	1.774	0.023	0.797
Weft genus	0.063	-	0.015	1.44	0.024	0.833

Correlation information is computed using the Pearson's moment correlation parameter for pairs of data taken at different locations i and i+k along the same tow spaced by kυ:

$$C_{auto}^{(j,t,p)}(k) = \frac{\sum_{i:=1}^{n-k} \delta\varepsilon_i^{(j,t,p)} \delta\varepsilon_{i+k}^{(j,t,p)}}{\sum_{i:=1}^{n-k} \left(\delta\varepsilon_i^{(j,t,p)}\right)^2 \sum_{i:=1}^{n-k} \left(\delta\varepsilon_{i+k}^{(j,t,p)}\right)^2} \qquad (2)$$

This coefficient is used to determine the correlation length ξ, defined as the slope of the straight line fitted to the correlation values, using data of small k:

$$C^{(j,t,p)}(k) \approx 1 - k\upsilon / \xi^{(j,t,p)} \quad (3)$$

This linear fit uses only the first five data points ($k \leq 5$). Higher spacing of points ($k>5$) are populated by much smaller data sets and are unreliable for estimating the correlation length.

The correlation lengths of the properties along the tow path, are shown in Table 3. The out-of-plane centroid possesses a correlation length in the range of 2-4 mm, while the in-plane centroid correlation length exceeds the unit cell dimensions. The in-plane component is less controlled than the out-of-plane centroid during RTM production where flat platens fix the thickness of the laminate. The area has a correlation length similar to the cross-over spacings, while the aspect ratio and orientation vary within the unit cell size.

Cross-correlations between tows of the same or different genuses are also investigated, but no significant correlation is found. Limited correlation, between 0.4 and 0.6, is found for respectively the in-plane component of neighbouring warp and weft tows.

Large uncertainty is present when deriving the correlation lengths using only data of the single plies, as shown in Figure 4 for the correlation of the z-centroid. The limited size of the data set for the largest point separations causes fitted lines to be affected by outliers, which is a major source of variability in the correlation length. Additional data must be collected to bring down this variation. For further details and discussion of the results is the reader referred to [9].

Table 3. Experimental correlation lengths

	ξ_x [mm]	ξ_y [mm]	ξ_z [mm]	ξ_{AR} [mm]	ξ_A [mm]	ξ_θ [mm]
ξ^{warp}	-	22.89	1.78	7.26	2.53	4.56
ξ^{weft}	9.42	-	1.62	5.48	1.01	3.49

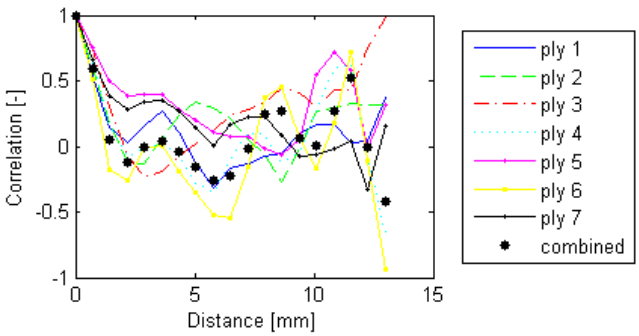

Figure 4. Correlation graph of the z-centroid for pairs of points along the tow using single-ply data only.

2.3 *Long range data*

The investigation of short range variations pointed out that only the in-plane centroid component of the tow path possesses a long range effect, indicated by the correlation length which exceeds the unit cell dimensions. Additional data on the long range are collected to complement this short range information. Two one-ply reinforcements, spanning a region of thirteen unit cells by thirteen unit cells, are produced in an RTM process. The production of one-ply samples is more challenging then multiple-ply samples but offers the advantage to obtain a high contrast between tow and resin regions for the image processing step.

Characterisation of the in-plane centroid is performed by optical imaging. A scan with a resolution of 1200 dots per inch is taken of the in-plane dimension (see Figure 5). The digital image is marked with a square region of 10 unit cells, away from the edges to minimise possible edge effects and large enough to be at least one order of magnitude larger than the sample used to collect the short range data. The freeware GIMP is used to extract the in-plane position of the 40 warp and 40 weft tows within the region of interest. Boundaries of the tows are marked based on visual recognition for prescribed grid spacings of 125 pixels in x (warp) and y (weft) direction. The centroid locations are subsequently defined as half the tow width at each grid location. These coordinates are given as input to Matlab where they are transformed to a global axis system and compensated for possible misalignment during scanning. A continuous representation of the discrete tow data is afterwards obtained by cubic spline interpolation.

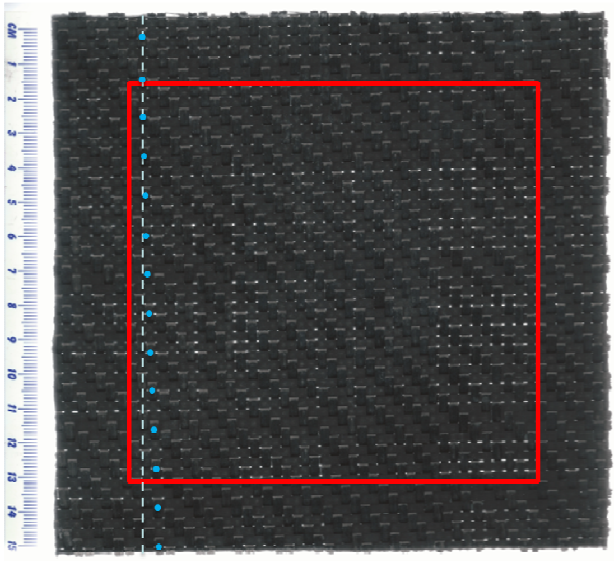

Figure 5. Optical scan of a one-ply 2/2 twill woven composite.

Figure 5 demonstrates that the in-plane centroid does not follow a straight path over the extent of the sample. The straight dotted line in the image starts at the same location of a tow of which the path is described by blue dots. When marching along the tow, a large deviation from the line is observed. These in-plane undulations are quantified by computing the difference between the experimental tow paths and an ideal lattice description. Tows of this lattice are represented as straight lines, with nominal spacing in x- and y-direction derived from the experimentally obtained unit cell periods. A best fit of this lattice with the experimental cross-

over locations of the tows is sought by a minimisation algorithm reducing the overall standard deviation of the fluctuations from the grid. The in-plane warp and weft fluctuations are considered respectively in y- and x-direction. This procedure is shown in Figure 6 with the deviations shown for the warp tows of sample 1 and 2. The obtained deviations can be represented as $\delta\varepsilon_i^{(j,t,s)}$ with i the grid location (i=1..N_i and N_i=40) , j the tow index (j=1..N_f and N_f=40) in each direction, t=warp or weft tows, and s=1 or 2 referring to the experimental sample.

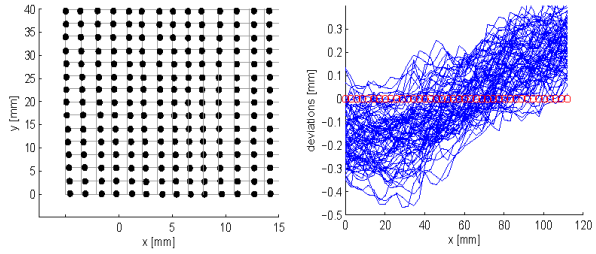

Figure 6. Defining the in-plane centroid deviations from a best fitted grid, applied to the warp tows.

These in-plane centroid fluctuations have a particular non-periodic trend. Similar to the reference period collation method, the deviations $\delta\varepsilon_i^{(j,t,s)}$ are further decomposed as expressed by equation 1, but with a different interpretation given to the terms. The lack of periodicity in the mean pattern, computed by considering the mean value per grid point $<\delta\varepsilon_i^{(j,t,p)}>$, signifies that this tendency should not be interpreted as a systematic trend, representing the repetitive mean behaviour of the tow path, but as an effect due to handling. Variability is already added to the in-plane centroid paths before production due to storage and handling of dry fabrics, e.g. unwinding of the fabric from the pulley and preparing the stacking sequence in the RTM mould. Subtraction of the handling trend from the deviation values $\delta\varepsilon_i^{(j,t,s)}$ per sample results in stochastic variations $\zeta_i^{(j,t,s)}$ which are attributed to the loom itself. The characterisation procedure of the long range in-plane variations can be summarised as:

$$\delta\varepsilon_i^{(j,t,p)} = \left\langle \delta\varepsilon_i^{(j,t,p)} \right\rangle + \zeta_i^{(j,t,p)} \tag{4}$$

The random behaviour of the in-plane deviations $\zeta_i^{(j,t,s)}$ is further described in terms of standard deviation and correlation length. Correlation of the centroid is considered along a single tow, further called auto-correlation, but also between neighbouring tows of the same type, named cross-correlation. The latter correlation type is significantly present for the long range data of the in-plane centroid, indicated by the bundling of tow positions in Figure 5, in contrary to the short range data where only a limited correlation value is observed.

The standard deviation σ for the combined data set of warp and weft tows are presented in Table 4. Although small differences between warp and weft in-plane centroids are obtained in the short range data, the current data show a significantly larger variation for the weft tows. This variability can be explained by the production process: warp tows are put under tension during fabrication of the fabric, while weft tows are inserted. Weft tows are therefore less restricted in their in-plane movement.

Table 4. Standard deviation of the in-plane centroid for the warp and weft tows.

	Sample 1	Sample 2	Combined
σ_{warp} [mm]	0.108	0.105	0.106
σ_{weft} [mm]	0.701	0.515	0.615

Correlation information is computed using the Pearson's moment correlation parameter (equation 2) for pairs of data or *lags* taken at distinct locations on a single tow, in the case of auto-correlation, or pairs of data taken at a single location at neighbouring tows, in the case of cross-correlation. A clear tendency is present in the correlation graphs, which together with the increased size of the data set permits to derive a representative correlation function. Each correlation structure is fitted with an exponential C_{exp} or squared exponential $C_{sq,exp}$ correlation function to estimate the correlation length ξ, with τ the lag spacing:

$$C_{\exp}(\tau) = e^{-\frac{|\tau|}{\xi}} \tag{5}$$

$$C_{sq,\exp}(\tau) = e^{-\frac{|\tau|^2}{\xi^2}} \tag{6}$$

Only these two types of function are considered since it is not the objective to find the optimal function perfectly representing the experimental correlation information, but to consider conventional functions which are physically reasonable. Each function is fitted in a least-square sense where the sum of squares of the residuals E_{res} at each lag between the experimental correlation data $c_{data,i}$ and the fitted correlation data $c_{fit,i}$ are minimised:

$$E_{res} = \sum_{i=1}^{N_i} \left(c_{data,i} - c_{fit,i} \right)^2 \tag{7}$$

Either the exponential or square exponential function is preferred with an error E_{res} less than or equal to 1%. Figure 7 shows the fitting procedure to the correlation information of the warp tows. The points in lighter grey are not considered for the fitting procedure due to (i) the small size of the data set for that lag location or (ii) zero-correlation is already reached. Negative correlation values are not used to derive the correlation length.

Table 5 presents the auto- and cross-correlation lengths obtained from exponential and squared exponential function fitting for the warp and weft tows using the combined data set: deviations of sample 1 and sample 2 are combined for each tow direction.

The warp auto- and cross-correlation information are well represented by an exponential correlation function C_{exp}. The correlation length along the warp tow spans ten unit cells. This value demonstrates the straightness of the warp tows,

which are kept straight during production. The observation of the cross-correlation data shows that a shift of the in-plane warp centroid only affects near-neighbouring tows within one unit cell distance.

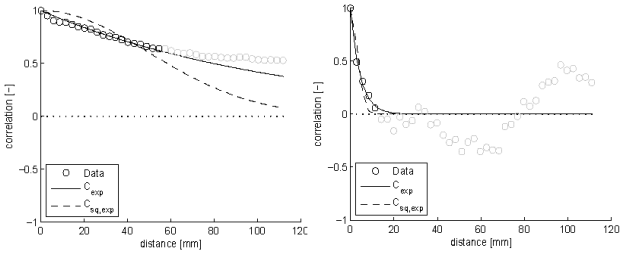

Figure 7. Auto- and cross-correlation graphs of the in-plane centroid of the warp tows.

The auto- and cross-correlation of the weft tows have a squared exponentional correlation behaviour $C_{sq,exp}$. In-plane deviations along the weft direction seem to persist between four and five unit cells. This corresponds to only half the warp auto-correlation length, caused by the larger variability in the weft tow path. The cross-correlation length of the weft tows shows an influence exceeding the unit cell size. Positions of the weft tows are less controlled due to the lack of tensioning during production. This affects near- and further-neighbouring tows causing the band behaviour to appear in the composite tow paths as shown in Figure 5.

Table 5. Correlation lengths along the tow and between neighbouring tows for the in-plane centroid.

	C_{exp} [mm]	E_{res}	$C_{sq,exp}$ [mm]	E_{res}
ξ_{auto}^{warp}	114.89	0.5%	70.03	8.9%
ξ_{cross}^{warp}	4.49	0.3%	4.55	6.8%
ξ_{auto}^{weft}	75.72	18.6%	52.89	1.0%
ξ_{cross}^{weft}	13.89	6.7%	13.16	0.6%

More information about the statistical characterisation of the in-plane centroid can be found in [12].

3 STOCHASTIC MULTI-SCALE MODELLING APPROACH

3.1 Overview

Virtual specimens are generated that possess the same statistical information as measured in the experimental samples. Realistic descriptions are obtained by using the experimental statistical information as input in the modelling strategy.

Each specimen is built by combining the experimental systematic and handling trends with zero-mean deviations. The systematic trends at the short-range and handling effect at the long-range are taken directly from the experimental data. The zero-mean stochastic deviations need to be generated such that they represent the sample standard deviation and correlation lengths for each tow parameter.

Different generator techniques are used to represent the full randomness of the tow reinforcement at the meso- and macro-scale. Tow path parameters which vary within the unit cell size (out-of-plane centroid, tow area and tow aspect ratio) with no cross-correlation are generated using a Monte Carlo Markov Chain algorithm for textile structures, recently proposed by Blacklock et al. [3]. Generation of the long-range in-plane centroid deviations requires a different approach due to the cross-correlation. For this purpose, a methodology described by Vorechovsky [6] is applied where series expansion methods based on Karhunen-Loève decomposition produce cross-correlated Gaussian random fields.

In this modelling approach, it is assumed that (i) the generation of the short range deviations can be performed independently from the long range deviations, and (ii) the short range deviations (out-of-plane centroid, area and aspect ratio) do not exhibit any type of long range dependencies for spacing of points larger than one unit cell.

3.2 Modelling auto-correlated deviations

The zero-mean deviations of the out-of-plane centroid, area and aspect ratio are generated using the Markov Chain algorithm described in [3]. The deviations are produced (i) independently for each tow parameter at the same grid location and (ii) also independently from any parameter value at neighbouring tows.

The algorithm is implemented in Matlab and uses as input the database of the deviation values, standard deviation and correlation length of each tow component. The deviations of each parameter is discretised on an interval with grid spacing a and number of intervals $2m+1$: $\{-ma, -(m-1)a, \ldots, 0, \ldots, (m-1)a, ma\}$ that satisfies the relation $ma=3\sigma_{\varepsilon}$. The parameter m is chosen to be 20. A lower value of m, and corresponding higher a, would result in (i) high amplitude of spikes in the produced deviations and (ii) unrealistic jumps in the centroids path for subsequent deviation values. The probabilities according to this discretised interval are collected in the distribution vector P_i for location i. The Markov process consists in generating the distribution vector P_{i+1} of the particular parameter at the next grid location $i+1$ using the probability transition matrix A:

$$P_{i+1}^{\varepsilon} = AP_i^{\varepsilon} \tag{8}$$

This probability matrix is tri-diagonal consisting of three parameters α,β,γ. The parameter α is given an arbitrarily fixed value of 0.9, while the relative magnitudes of the parameters β and γ are varied to ensure that the procedure results in the same standard deviation and correlation length on average as derived experimentally. Each tow parameter has its own $(2m+1)$ by $(2m+1)$ probability transition matrix. The Markovian procedure is the core computation of the Monte Carlo based operating algorithm which is repeated for all parameters.

The produced deviations possess high-amplitude long range wavelength fluctuations, similar to the correlation length of the considered parameter, combined with low-amplitude short range wavelength variations. The latter effect can appear as unphysical sharp spikes which are not present in the

experimental sample. A smoothing operation is required to reduce the amount of spikes using an averaging procedure without affecting the statistics of the deviations too much. An adapted version of the moving box average is used for this purpose that conserves the standard deviation [3]. Deviation values are smoothed using information of ± 2 neighbouring grid points. The smoothing operation is demonstrated in Figure 8 for the generated z-centroid deviations.

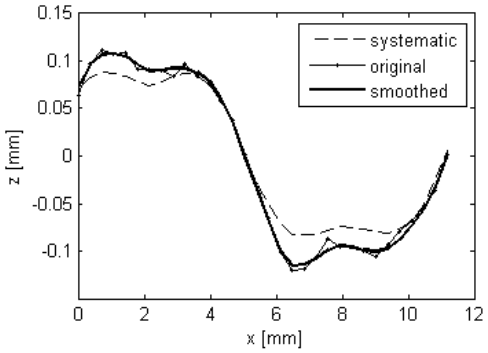

Figure 8. Generated out-of-plane centroid deviations for a single tow using the Markov Chain algorithm.

The generation procedure is validated by generating 4000 warp and weft tow deviations. The produced standard deviations are compared with the experimental data of the combined data set, while the simulated correlation lengths are checked with the mean values of the experimental correlation lengths, derived using the single-ply data set.

Generated standard deviations and correlation lengths of the out-of-plane centroid coordinate are given as example in Figure 9 for non-smoothed and smoothed deviations. The produced standard deviations are centered around the experimental standard deviation. The smoothing operation slightly affects the out-of-plane centroid. In the case that one or more points in the averaging interval have a different sign, the conventional smoothing procedure must be applied which does not conserve the standard deviation.

A high variance is observed for the generated correlation lengths, for non-smoothed and smoothed results. The sensitive calculation of the correlation length as linear approximation of the first lags in the autocorrelation graph results in significant variability. The additional smoothing step shifts the correlation length values to the more positive values, which is expected since neighbouring values are made more by the smoothing process. However, the magnitude of the smoothed correlations remains the same. Figure 9 presents the obtained statistical information for the out-of-plane position. This process is repeated for all tow properties.

Table 6. Standard deviation and correlation length of the generated warp z-centroid.

	σ_z [mm]	ξ_z [mm]
Warp genus - *no smoothing*	0.014	2.26
Warp genus - *with smoothing*	0.013	3.57

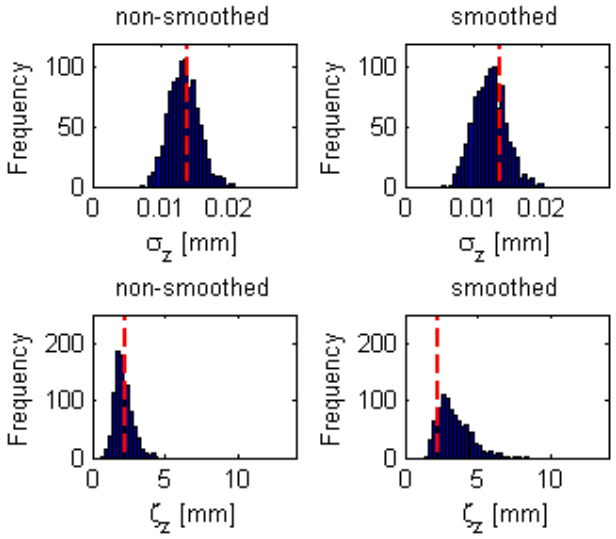

Figure 9. Simulated standard deviations and correlation lengths of the out-of-plane centroid for 1000 different unit cells. Red dashed line indicates the experimental mean value.

Random unit cell structures of the 2/2 twill woven composite are already successfully generated using this methodology in [10], with data for the in-plane centroid taken from the short range data set. After combining the systematic trends with the produced deviations of each tow parameter, the random reinforcement structure is introduced in the WiseTex software [8]. The discrete tow information of a 2/2 twill woven norminal WiseTex model is overwritten with the updated tow path, while other fibre and matrix properties are maintained. An arbitrary virtual specimen is presented in Figure 10.

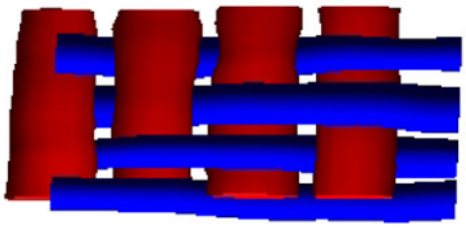

Figure 10. Virtual random unit cell structure presented in the WiseTex format.

3.3 Modelling auto- & cross-correlated deviations

Since the in-plane centroid deviations are correlated along the tow and between neighbouring tows, a different approach is required to simulate deviations having the experimental target statistics. The deviations for this centroid component must be produced simultaneously for all tows of the same genus in order to model the cross-correlation correctly. A methodology proposed by Vorechovsky [6] is applied where series expansion methods based on Karhunen-Loève decomposition produce cross-correlated Gaussian random fields. The procedure is originally used to simulate random fields of metal properties, such as Young's modulus and Poisson coefficient, which are cross-correlated. The assumptions that (i) all cross correlated fields must share an

identical auto-correlation structure and (i) the cross-correlation structure between each pair of correlated fields can be defined by a cross-correlation coefficient, are also valid for woven textile structures. In-plane positions of each tow within a virtual specimen are modelled as Gaussian random fields where tows belonging to the same genus share an identical auto-correlation structure and are cross-correlated at the same time with neighbouring tows of the same type.

The method is based on modal decomposition of the correlation matrices. In a first step the eigenvalues and eigenvectors of the auto-correlation and cross-correlation matrix are determined. The same spectrum of eigenvalues λ^A and eigenvectors Φ^A of the auto-correlation is applied for all cross-correlated fields. The eigenvalues λ^C and eigenvectors Φ^C of the cross-correlation matrix are used to transform the independent, uncorrelated random variables η, needed to construct all one-dimensional Gaussian fields of the virtual specimen, into cross-correlated random values χ:

$$\chi = \phi^C \lambda^C \eta \tag{9}$$

It is recommended to use Latin Hypercube Sampling (LHS) to simulate the random variables η. The vector χ has deviations which are uncorrelated along a single field and cross-correlated between fields. It can be decomposed in blocks χ_i where each block *i* delivers the random variables used in the one-dimensional Karhunen-Loève expansions to represent a single tow in the virtual specimen. Possible spurious correlation along the random variables χ_i of a field can be diminished using correlation control techniques [11]. The random field H_i of each tow is represented as:

$$H_i(x,\theta) = \sum_{j=1}^{N_{var}} \sqrt{\lambda_j^A}\, \chi_{i,j} \phi_j^A(x) \tag{10}$$

with N_{var} the number of eigenmodes used to represent the variability after truncation. Truncation of the series expansion can be considered in order to reduce the computational cost. For more details the reader is referred to [6].

The in-plane position of the 2/2 twill woven composite is simulated, using the fitted correlation functions as target correlation structures in combination with the experimental standard deviation. No correlation control techniques are considered to reduce possible spurious correlation between the random variables χ_i. A sensitivity analysis concluded that this additional operation does not add a significant difference in the resulting statistics. Omitting such operation significantly downsizes the computational expense.

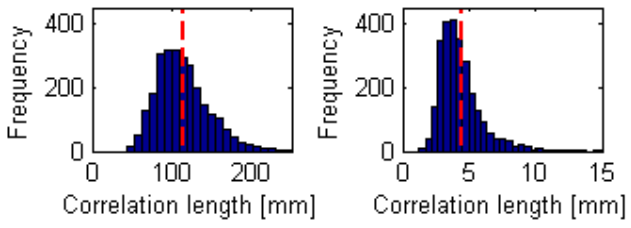

Figure 11. Simulated auto- (left) and cross-correlation (right) lengths. Red dashed line indicates the experimental mean.

Warp in-plane centroids are computed by applying truncation of the series expansion for the auto-correlation. Only 33 of the largest eigenvalues and corresponding eigenvectors are considered instead of 40, given an acceptable truncation error of 0.25% (99.75% of the variability is captured). No reduction is applied for the cross-correlation. Results demonstrate good agreement for standard deviation and correlation information of the entire field as shown in Figure 11 for the simulated auto- and cross-correlation lengths. The simulations of the in-plane centroid achieve the statistical information on average considering all the tows of the specimen, as quantified in Table 7 for the warp tows.

Table 7. Simulated statistics for the warp in-plane centroid.

	Simulated mean [mm]	Target mean [mm]
mean	2.25E-6	0
σ	0.1025	0.1063
ξ_{auto}	113.73	114.89
ξ_{cross}	4.36	4.49

However, when only data of the single tows are considered a higher mean auto-correlation length is obtained but within the same order of magnitude as presented in Figure 12**.** The dissimilarity in correlation information per single tow can be attributed to the fact that the derivation of the correlation length is subjected to a large uncertainty. This property is obtained as a result of fitting exponential curves of which the correlation length is the denominator (see equation 5 and 6). Essentially this means that a different correlation length results in another curvature of the exponential function. This process is extremely sensitive to small deviations. As mentioned in section 2.2, is the limited size of the data set for large point separations the major source of variation since it is affected by outliers. A wide scatter in the correlation lengths is gained as already shown in Figure 12**.**

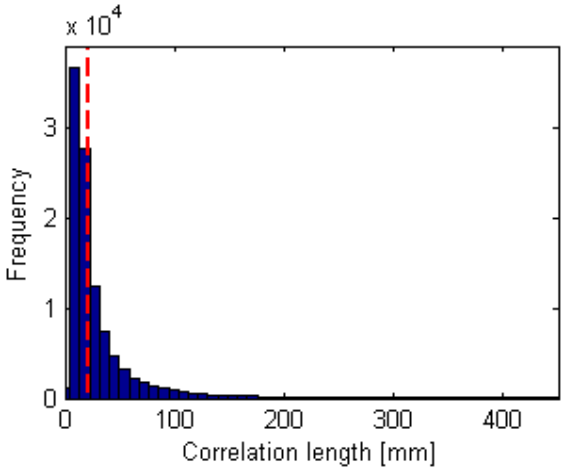

Figure 12. Simulated auto-correlation lengths of individual warp tows. Red dashed line indicates the experimental mean.

Zero-mean deviations are obtained which do not require any smoothing operation. Short range fluctuations of the in-plane centroid are not spiked when using series expansion techniques and long range variations are comparable to the target correlation length.

4 DISCUSSION

The next step in the generation of multiple unit cell structures is combining the simulated deviations possessing short range variations (out-of-plane centroid, aspect ratio and area) with the longer range in-plane positional fluctuations. The random multiple unit cell structures are thereafter introduced in the WiseTex format [8] to represent the virtual specimens. More details and results of this generation of multiple unit cell structures is ongoing work and will be addressed in future publications.

The realistic representations of internal geometry can be applied to (i) improve the understanding of damage propagation in textile composites and (ii) quantify the spatial variation of the mechanical properties over composite components, such as stiffness, caused by variation in the reinforcement structure.

In exception of the in-plane centroid, all tow path parameters are generated independently from its neighbouring tows. This approach can lead to interpenetration between tows belonging to the same genus, but also for tows belonging to a different genus at locations such as the cross-over points. Although stiffness computed with Mori-Tanaka is not affected by interpenetration of tows, the model requires small adaptations when the WiseTex model is transformed into a finite element model. Tows need to be translated but such that topological rules stay satisfied [5,7].

5 CONCLUSIONS

Virtual specimens of a 2/2 twill woven composite produced by RTM are generated which possess the same statistical information as measured from experimental samples.

In a first step, experimental data are collected where each tow property is characterised in terms of mean value along the tow path, standard deviation and correlation information. The mean value shows a repetitive periodic trend for the out-of-plane centroid, area and aspect ratio, which is correlated with the cross-over locations. A non-periodic long range trend is observed for the in-plane coordinate reflecting the handling effect of the fabric. The in-plane coordinate is also subjected to the largest variation, described by the standard deviation, with a correlation length along the tow spanning ten unit cells on average for warp direction and approximately five for weft direction. It is also the only property of the tow path which is cross-correlated with neighbouring tows of the same type, reaching around one unit cell distance. Out-of-plane centroid and tow cross-sectional properties vary within the unit cell size, with area and aspect ratio strongly dependent with the cross-over locations. No cross-correlation is observed for these properties.

Next, statistical information is given as input to a stochastic multi-scale modelling approach where the mean patterns are taken from the experimental information and deviations are generated possessing the target statistics. The tow parameters without cross-correlation are generated with a Monte Carlo Markov Chain, while the cross-correlated in-plane centroid is produced based on Karhunen-Loève expansions. All simulated tow deviations achieve the target statistics. Combination of the mean trends with the produced deviations for each tow property results in random woven structures which represent the internal geometry variability throughout composite samples.

ACKNOWLEDGMENTS

This study is supported by the Flemish Government through the Agency for Innovation by Science and Technology in Flanders (IWT) and FWO-Vlaanderen.

REFERENCES

[1] Hexcel, HexForce G0986 SB 1200, USA, 2012.

[2] H. Bale, M. Blacklock, M. Begley, B. Cox and R. Ritchie, "Characterizing three-dimensional textile ceramic composites using synchrotron X-ray micro-computed-tomography," *Journal of the American Ceramic Society,* vol. 95, pp. 392-402, 2012.

[3] M. Blacklock, H. Bale, M. Begley and B. Cox, "Generating virtual textile composite specimens using statistical data from micro-computed tomography: 1D tow representations for the binary model," *Journal of the Mechanics and Physics of Solids,* vol. 60, no. 3, pp. 451-470, 2012.

[4] D. C. Charmpis, G. I. Schuëller and M. F. Pellisetti, "The need for linking micromechanics of materials with stochastic finite elements: a challenge for materials science," *Computational Materials Science,* pp. 27-37, 2007.

[5] S. V. Lomov, D. S. Ivanov, I. Verpoest, M. Zako, T. Kurashiki, H. Nakai and S. Hirosawa, "Meso-FE modelling of textile composites: road map, data flow and algorithms," *Composites Science and Technology,* vol. 67, no. 9, pp. 1870-1891, 2007.

[6] M. Vorechovsky, "Simulation of simply cross correlated random fields by series expansion methods," *Structural Safety,* vol. 30, no. 4, pp. 337-363, 2008.

[7] R. G. Rinaldi, M. Blacklock, H. Bale, M. R. Begley and B. N. Cox, "Generating virtual textile composite specimens using statistical data from micro-computed tomography: 3D tow representations," *Journal of the Mechanics and Physics of Solids,* vol. 60, no. 8, pp. 1561-1581, 2012.

[8] I. Verpoest and S. V. Lomov, "Virtual textile composites software WiseTex: integration with micro-mechanical, permeability and structural analysis," *Composites Science and Technology,* vol. 65, no. 15-16, pp. 2563-2574, 2005.

[9] A. Vanaerschot, B. N. Cox, S. V. Lomov and D. Vandepitte, "Stochastic framework for quantifying the geometrical variability of laminated textile composites using micro-computed tomography," *Composites Part A,* vol. 44, pp. 122-131, 2013.

[10] A. Vanaerschot, B. N. Cox, S. V. Lomov and D. Vandepitte, "Stochastic multi-scale modelling of textile composites based on internal geometry variability," *Computers & Structures,* vol. 122, pp. 55-64, 2013.

[11] M. Vorechovsky and D. Novak, "Correlation control in small-sample Monte Carlo type simulations I: A simulated annealing approach," *Probabilistic Engineering Mechanics,* vol. 24, pp. 452-462, 2009.

[12] A. Vanaerschot, B. N. Cox, S. V. Lomov and D. Vandepitte, "Statistical characterisation of the in-plane tow centroid in textile composites to quantify the multi-scale variation in geometry," in *Proceedings of the IUTAM Symposium on Multiscale modeling and uncertainty quantification of materials and structures*, Santorini, 2013.